27

Recovery of Biosynthetic Products Using Membrane Contactors

Carlo Gostoli
Department of Chemical Engineering, Alma Mater Studiorum – University of Bologna
Italy

1. Introduction

Membrane Contactors (MC) make possible to accomplish gas-liquid or liquid-liquid mass transfer operations without dispersion of one phase within another. The membrane acts as a mere physical support for the interface and does not contribute to the separation through its selectivity, the separation being primarily based on the principle of phase equilibrium.
Porous membranes with narrow pore size (typically in the range 0.02-0.2 μm) are used. One of the two phases enters the membrane pores and contacts the other phase at the pore mouth on the opposite side. Generally MC operations involve an aqueous phase and the membrane has hydrophobic character, however hydrophilic membranes can be used too [Kosaraju & Sirkar, 2007]. The key factor is that one of the two phases enters the pores whereas the other phase is kept outside. In the case of hydrophobic materials (Fig. 1), the membrane pores are filled by the non-polar phase or by the gas while the aqueous phase can not penetrate into the pores.

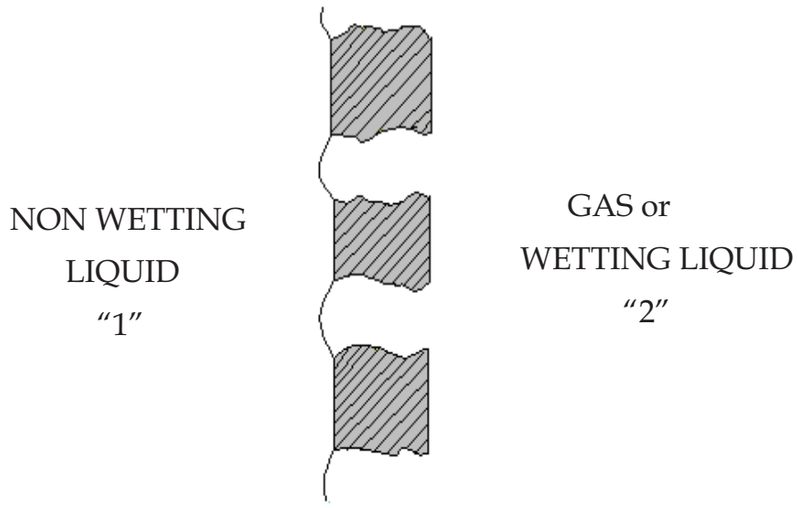

Fig. 1. The membrane contactor concept based on porous hydrophobic membrane in contact with an aqueous (non wetting) liquid at one side and a gas or organic (wetting) liquid at the other side

It is worth noting that the hydrophobicity of the materials is not a warranty for keeping the aqueous phase outside of the pores, indeed if a critical pressure value, called *breakthrough pressure*, is exceeded, the aqueous phase enters the membrane pores. The *breakthrough pressure* depends on the maximum pore size, d_P, the interfacial tension between the two phases, γ, the contact angle between the membrane and the two fluid, θ, according to the Young-Laplace equation (strictly valid for cylindrical pores):

$$\Delta P_c = \frac{4\gamma|\cos\theta|}{d_P} \tag{1}$$

As a consequence it is important to carefully control the operating pressures: the pressure of the aqueous phases has to be a bit higher than the pressure of the organic/gas phase, but lower than the breakthrough pressure. Selecting appropriate membrane materials and pore size it is possible to assure a pretty wide range of pressure for safe operations, for example PTFE or polypropylene membranes with nominal pore size of 0.2 μm exhibit a breakthrough pressure of nearly 3 bars for the water-air system. The discussion above can be extended to hydrophilic membranes; in that case the pores are filled by the aqueous phase, whose pressure has to be taken a bit lower than the gas/organic phase pressure, which in turn has to not overcome the breakthrough pressure, given again by Eq. (1). The choice between hydrophobic and hydrophilic membranes is dictated by the need to reduce the membrane resistance. As a rule the membrane pores should be filled by the phase in which the transferred species is most soluble. For example, if the species has higher affinity with the non polar or gas phase hydrophobic membrane will be preferred. If there is higher affinity with the polar phases the membrane will be hydrophilic.

MC have many advantages with respect to conventional mass transfer apparatuses: - membrane modules, in the form hollow fibres, provide interface areas per unit volume significantly greater than traditional devices, leading to more compact systems, - the interfacial area is well defined and remains constant regardless of the flow rates, whereas the design of the conventional devices is restricted by limitations in the relative flows of the two streams. - there is no mix of the two phases separate by the membrane and thus no need to separate the two phases downstream the process and no need of difference of density. - In addition MCs are easy in scale up and control, modular in design, flexible in operation.

Membrane contactors can be used for carrying out the recovery of bioconversion products from aqueous solutions by organic solvents, usually conduct in centrifugal devices, mixer-settler or columns. An additional advantage is relevant in this case: the operation can be performed in the presence of the living cells or enzymes that indeed do not get in direct contact with the solvent. The use of membrane based, dispersion free, solvent extraction for the recovery of bio-products, pioneered by Sirkar [Frank & Sirkar, 1987] has been well documented [Gawronski, 2000; Lazarova et al., 2002; Schlosser al., 2005].

Of course MCs present also some disadvantages: - no doubt the membrane represents an additional mass transfer resistance, and indeed overall mass transfer coefficients lower than those of conventional devices have been reported. However this drawback is well offset by the larger specific area, as a consequence the volumetric mass transfer coefficient for MCs is well above the values achievable in conventional devices. As in other membrane processes, problems my be the limited life time and fouling. However fouling my be less severe than in pressure driven processes; suspended solids and solutes are indeed not forced into the pores by convective flow, the species being transferred from one phase to the other by only diffusion.

2. Membrane and modules

Polymeric membranes were usually employed in membrane contactor studies and applications, because they are very competitive in performance and economics. Membranes with high hydrophobicity were preferred in most applications. Polypropylene (PP), polytetrafluoroethylene (PTFE), and polyvinylidenefluoride (PVDF) have been extensively used. Among these, microporous PTFE membrane shows excellent performance and stability, however, the application on industrial scale is limited, since PTFE membranes are available in flat sheet form rather than as hollow fibres. At present hollow fibre PP membranes exhibit the widest applications due to the good thermal and chemical stability, well-controlled porosity, and low cost. Recently increasing efforts have been devoted to develop ceramic membranes [Koonaphapdeelert et al., 2007, 2009; Li, 2007.], or hybrid membranes to get better chemical and thermal stability as well as higher mechanical strength. Membrane surface modification techniques to improve the hydrophobicity has also been investigated [Lv et al., 2011].

In principle both flat sheet membranes and hollow fiber can be used to make MC apparatuses. Fig. 2 shows the concept of a plate and frame module: it contains parallel membrane sheets with interposed spacers. Problems can arise from the susceptibility of the membrane to mechanical abrasion that required a careful design of the spacers and/or the use of supported membrane with an active layer, made for example of PTFE, and a woven or unwoven fabric. In this case the spacer in the active layer side can be substituted by a simple frame. Co-current flow is to be preferred to counter-current flow, in order to have a nearly constant pressure difference along the membrane, avoiding pressure inversion and membrane movement.

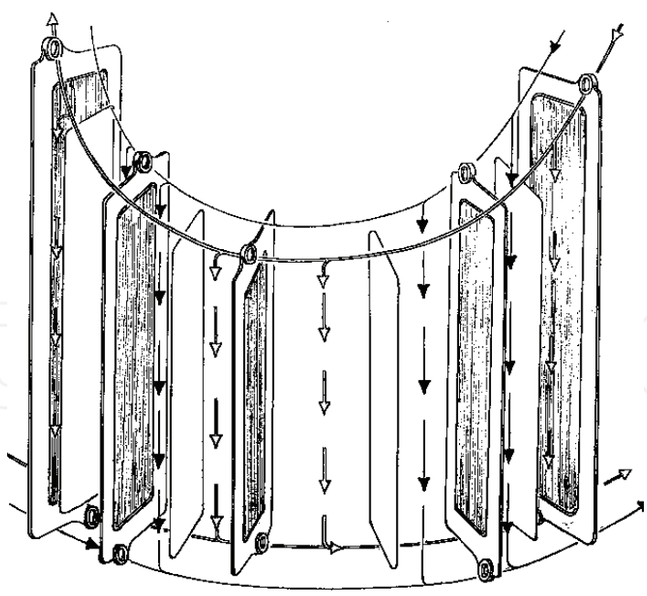

Fig. 2. The concept of plate & frame membrane contactors

The membrane area, a, per unit volume of these apparatuses is quite limited; assuming for example 1 mm the thickness of the fluid channels and 2 mm the thickness of the frames, the membrane area is a = 250 m^2/m^3 . Taking into account the borders and the manifolds,

membrane area similar to or lower than conventional apparatuses can be estimated, so the main advantage of MC is lost. Plate and frame MC can be considered for particular applications, for example in air conditioning systems [Gaeta, 2003.], to reduce the pressure drop, or in the treatment of liquids containing suspended solids. Also spiral wound configuration has been proposed [Koschilowski et al., 2003].
Notwithstanding the larger availability of flat sheet membrane and its larger permeability, hollow fibers are generally preferred due to their high packing density. The basic hollow fibre module configuration with parallel flow of the streams is represented in Fig. 3. More complex configurations have been conceived in order to improve the mass transfer rate, as an example by inducing cross flow in the shell side [Drioli et al., 2006].

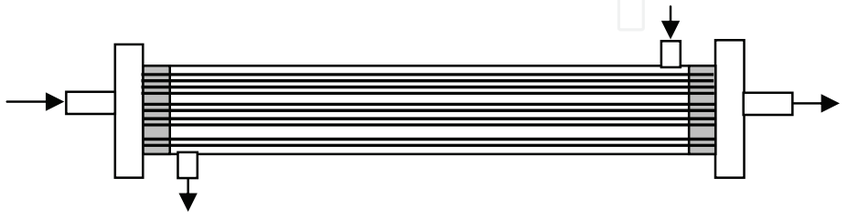

Fig. 3. Hollow fibre module

The fibre packing density can be characterized by the packing fraction, ϕ, representing the fraction of the cross section of the module occupied by the fibres. Denoting by N the number of fibres, d_o their outer diameter and d_S the shell diameter, we have:

$$\phi = N\left(\frac{d_o}{d_s}\right)^2 \tag{2}$$

Sometime the void fraction $\varepsilon = 1-\phi$ is used instead to characterize the packing density of the fibre bundle. The inner and outer membrane areas per unit volume (a_i and a_o respectively) are simply related to the packing fraction and diameters:

$$a_i = \frac{4\phi d_i}{d_o^2} \qquad a_o = \frac{4\phi}{d_o} \tag{3}$$

In order to give an estimation of the membrane area per unit volume achievable with hollow fibres, let's consider a regular triangular arrangement of fibres with pitch 2s (Fig. 4). The cross section of the module appears formed by equilateral triangles of area $s^2\sqrt{3}$; each triangle contains 3/6 of circle, that's to say $3/6\pi d_i$ arc length, referring to the inner diameter, or $3/6\pi d_o$ referring to the outer diameter. The inner and outer membrane areas per unit volume are thus:

$$a_i = \frac{\pi}{2\sqrt{3}}\frac{d_i}{s^2} \qquad a_o = \frac{\pi}{2\sqrt{3}}\frac{d_o}{s^2} \tag{4}$$

Or, referring to the dimensionless pitch:

$$\sigma = \frac{2s}{d_o} \tag{5}$$

$$a_i = \frac{2\pi}{\sqrt{3}\sigma^2}\frac{d_i}{d_o^2} \qquad a_o = \frac{2\pi}{\sqrt{3}\sigma^2}\frac{1}{d_o} \tag{6}$$

For a given pitch to diameter ratio, σ, the membrane area per volume is thus in inverse relation to the fibre size d_o, and very large areas can be obtained by narrow hollow fibres.

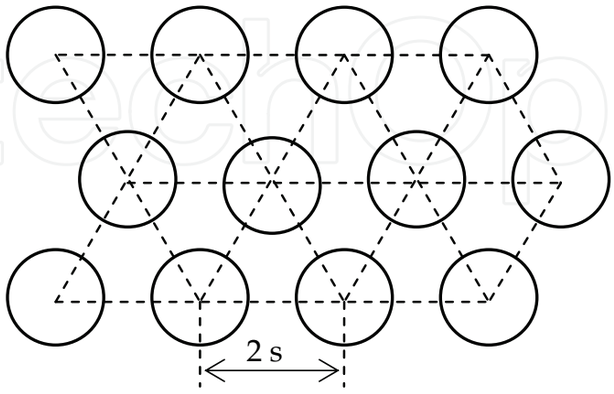

Fig. 4. Triangular array of fibres

Of course the maximum area is obtained when the fibres touch each other, i.e. for σ = 1. More realistic situations correspond to σ values about 1.5, for which the gap between the fibres is equal to the fibre radius. Tab. 1 reports the values of ai and ao achievable in triangular pitch with σ = 1.5, in hypothetical modules made with two well known, commercial PP hollow fibres.

	d_o mm	d_i mm	a_i m^2/m^3	a_e m^2/m^3
Accurel 0.6	1	0,6	967	1612
Celgard X40	0.3	0.2	3582	5373

Table 1. Membrane area per unit volume of modules made with Accurel or Celgard hollow fibres with pitch to diameter ratio σ = 1.5 (ϕ = 0.4)

Pitch of the triangular array and packing fraction are related by:

$$\phi = \frac{\pi}{2\sqrt{3}\sigma^2} \tag{7}$$

In particular the maximum packing, corresponding to σ = 1, is ϕ = 0.9, while σ =1.5 corresponds to ϕ = 0.4. Of course in commercial modules the hollow fibres are not arranged according to the regular array, as assumed above for illustrative purpose, however packing fraction in the range 0.4 – 0.5 are common and membrane area per unit volume are quite close to the values reported in Tab. 1.

3. Module design and module efficiency

Fig. 5 represents a counter-current mass transfer apparatus in which a species is extracted from an aqueous phase of flow rate W by a solvent of flow rate S. The flux N (*mol/m²s*)

across the interface in a section of the module in which the concentrations of the two streams are C_w and Cs is:

$$N = K_w(C_w - C_S / m) \tag{8}$$

in which K_w is the overall mass transfer coefficient based on the aqueous phase and m the partition coefficient.

$$m = \left[\frac{C_S}{C_w}\right]_{eq.} \tag{9}$$

For hollow fibres modules the flux can be referred to either the inner or outer surface of the fibres, provided that the mass transfer coefficient is defined accordingly.

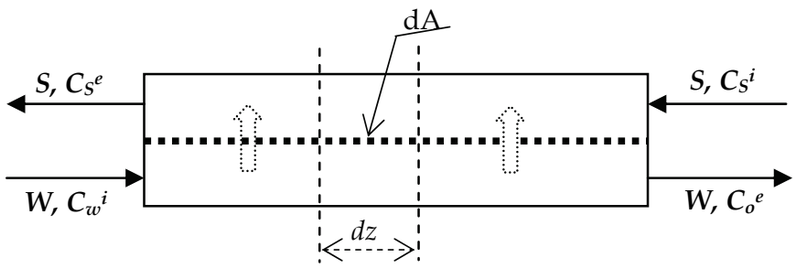

Fig. 5. Schematic of counter-current mass transfer apparatus. W and S are the flow rates of the aqueous and organic phases, C_w and C_S the respective concentrations

The design of the module is straightforward: we make a mass balance for the *dz* element of area *dA* (see Fig. 5):

$$W\frac{dC_w}{dA} = -K_w\left(C_w - C_S / m\right) \tag{10}$$

The membrane area A can be either the inner or outer surface of the fibres, as stated above. Since both Cw and Cs depend on the axial coordinate we must relate C_S to Cw, by the overall mass balance:

$$C_S = C_S^e + \frac{W}{S}\left(C_w^i - C_w\right) \tag{11}$$

After substitution and integration we have the membrane area:

$$A = \frac{W}{K_w}\frac{E}{E-1}\ln\frac{mC_w^i - C_S^e}{mC_w^e - C_S^i} \tag{12}$$

in which:

$$E = \frac{mS}{W} \tag{13}$$

represents the extraction factor.

Eq. (12) is useful in design problems, in which the inlet and exit concentrations of the two streams are given. When instead the module properties are given and we want relate the exit concentrations to the inlet ones, it is useful to introduce the module efficiency, defined as the ratio between the actual mass transfer occurring in the module and the maximum mass transfer corresponding to equilibrium between the water exit stream and the inlet solvent:

$$\eta = \frac{C_w^i - C_w^e}{C_w^i - C_S^i / m} \tag{14}$$

The efficiency is useful since it allows relating the overall amount of the species transferred to the inlet concentrations of the two streams. By a procedure similar to that followed above to obtain Eq. (12), the efficiency can be related to the overall mass transfer coefficient and membrane area:

$$\eta = \frac{1 - \mathrm{Exp}\left[-\frac{K_w A}{W}\left(1 - 1/E\right)\right]}{1 - \frac{1}{E}\mathrm{Exp}\left[-\frac{K_w A}{W}\left(1 - 1/E\right)\right]} \tag{15}$$

It is worth noting that efficiency approaches unity as the area goes to infinity, only if E > 1, while instead it approaches E if E < 1. Indeed in the former case the exit concentration of the aqueous stream approaches the value of equilibrium with the inlet solvent, whereas if E < 1, the exit concentration of the solvent approaches the value of equilibrium with the inlet aqueous stream. Finally Eq. (15) does not hold for the particular case of E = 1, in this case:

$$\eta = \frac{KA/W}{1 + KA/W} \tag{16}$$

Similar expression can be obtained for of co-current operation; in this case the efficiency, defined again by Eq. (14), is:

$$\eta = \frac{1 - \mathrm{Exp}\left[-\frac{K_w A}{W}\left(1 + 1/E\right)\right]}{1 + 1/E} \tag{17}$$

Of course co-current operation gives lower efficiency than counter-current operation.

3.1 Modelling of batch operation

In laboratory experiments, the membrane contactor and the reservoirs are usually arranged in closed system, in which the aqueous feed and the solvent are circulated through the module and the respective reservoirs, as represented in Fig. 6. Perfect mixing in the reservoirs and plug flow through the module are usually assumed. Apparently the system operates in unsteady state: the concentration of the aqueous phase, C_w, and the concentration of the organic phase, C_S, in the reservoirs change in time and eventually reach the equilibrium values corresponding to the partition coefficient. The module itself operates

in unsteady state, since the inlet concentrations are at any time equal to the concentrations prevailing in the reservoirs. Nevertheless, if the reservoir volumes are much larger than the module volume, or equivalently, the residence time in the module is negligible in the time scale of the experiment, the module can be considered to work in steady state, while the reservoirs work in unsteady state. This approach has been called pseudo steady state approximation and has been extensively used to analyze experiments intended to evaluate the overall mass transfer coefficient between the phases [D'Elia et al., 1986, Trébounet et al., 2006].

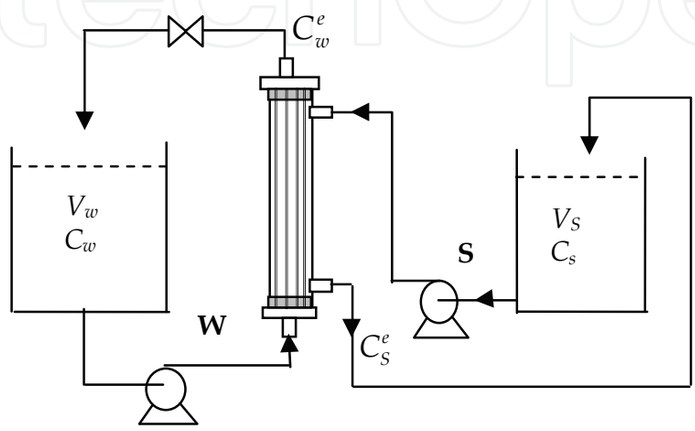

Fig. 6. Typical set-up of MC experiments

Based on the definition of module efficiency, Eq. (14), since the concentrations of the two streams entering the module are equal to the concentrations prevailing in the two reservoirs, the following mass balance equations hold, under the hypothesis of pseudo steady state:

$$V_w \frac{dC_w}{dt} = -W\eta\left(C_w - C_S / m\right) \tag{18}$$

$$V_w\left(C_w^0 - C_w\right) = V_S\left(C_S - C_s^0\right) \tag{19}$$

In principle V_w and V_S represent the volume of the two reservoir, but a better approximation is obtained considering V_w and V_S as total volumes of the two phases, comprehensive of the module and pipes volumes, even if these latter are generally quite small [Trébounet et al., 2006]. After integration and rearrangement we have:

$$\ln\frac{\left(1+1/R\right)C_w - C_w^0/R - C_S^0/m}{C_w^0 - C_S^0/m} = -\left[\frac{W\eta}{V_w}\left(1+\frac{1}{R}\right)\right]t \tag{20}$$

which in the case of extraction with initially pure solvent (C_S^0=0) simplifies to:

$$\ln\left[\left(1+\frac{1}{R}\right)\frac{C_w}{C_w^0} - \frac{1}{R}\right] = -\left[\frac{W\eta}{V_w}\left(1+\frac{1}{R}\right)\right]t \tag{21}$$

in which

$$R = \frac{mV_S}{V_w} \tag{22}$$

represents a sort of extraction factor for the whole operation, defined making reference to the phase volumes instead of stream flow rates, as in Eq. (13).
If the overall mass transfer coefficient as well as the volumes, flow rates and membrane area are known, we can calculate the module efficiency through Eq. (15), then the concentration of the aqueous phase vs. time through Eq. (20):

$$C_w = \frac{1}{R+1}\left\{\frac{C_w^0}{R} + \frac{C_S^0}{m} + \left(C_w^0 - \frac{C_S^0}{m}\right) Exp\left[-\frac{W\eta}{V_w}\left(1+\frac{1}{R}\right)t\right]\right\} \tag{23}$$

and eventually the concentration of the organic phase through Eq. (19).

$$C_S = C_s^0 + \frac{V_w}{V_S}\left(C_w^0 - C_w\right) \tag{24}$$

Alternatively the model can be used to evaluate the overall mass transfer coefficient from experiments. In this case the concentration of the two steams are measured vs. time, then the left side of Eq. (20) is plotted vs. time; from the slope of the straight line obtained we have the efficiency, eventually the mass transfer coefficient is calculated from eq. (15). The procedure has been reported in more details in the experimental section.

4. Mass transfer in hollow fibre contactors

Mass or heat transport for laminar flow in various geometries and under various boundary conditions was investigated by several authors, beginning with the classical work of Graetz for heat transfer in circular ducts with constant wall temperature [Knudsen & Katz, 1958]. Reference can be made to the work of [Siegel et al, 1958] for heat transfer in circular duct with uniform heat flux, [Hatton & Quarmby, 1962] for annular ducts and [Nunge and Gill, 1966] for a tube in tube heat exchanger. Various papers deal with haemodialysis in hollow fibre, for example [Davis & Parkinson, 1970; Gostoli & Gatta, 1980; Ding 2004].
The correct modelling of mass transfer in membrane contactors would require the simultaneous integration of the mass balance equations for the lumen and for the shell sides, the boundary conditions being equal flux at the membrane-fluid interfaces. However it is common practice to evaluate separately the individual mass transfer coefficients and to combine it in an overall mass transfer coefficient according to the resistance in series concept. The overall mass transfer coefficient embodies three contributions related to the tube and shell side boundary layers and to the diffusion through the membrane pores. Making reference to hydrophobic membranes, Eq. (25) holds in the case of aqueous feed flowing through the lumen:

$$\frac{1}{K_w} = \frac{1}{k_w} + \frac{1}{mk_m}\frac{d_i}{d_{lm}} + \frac{1}{mk_S}\frac{d_i}{d_0} \tag{25}$$

whereas for aqueous phase flowing through the shell we have:

$$\frac{1}{K_w} = \frac{1}{k_w} + \frac{1}{mk_m}\frac{d_0}{d_{lm}} + \frac{1}{mk_S}\frac{d_0}{d_i} \tag{26}$$

In both equations the mass transfer is referred to the actual interface: the inner surface of the fibres in the first case and the outer surface for aqueous feed flowing through the shell side.
Since in any case the membrane pores are filled by stagnant solvent, the mass transfer coefficient through the membrane is:

$$k_m = \frac{2D\varepsilon}{(d_0 - d_i)\tau} \tag{27}$$

Where ε is the membrane porosity, defined as the ratio between the cross sectional area of the pores and the total membrane area , and τ the tortuosity factor, taking into account that the diffusion path is longer than the membrane thickness due to the pores geometry. Typical values of tortuosity for the membranes mostly used are around 2. The diffusion coefficient, D, of the species in the solvent, if not available, can be estimated by predictive methods, for example the Wilke-Chang equation [Reid et al., 1978]. Mass transfer coefficients can be also evaluated experimentally by the Wilson plot method [Seara et al., 2007].

4.1 Mass transfer in hollow fibre lumen

The calculation of tube side mass transfer coefficient is well established, in that it represents the classical Graetz problem. Solutions are presented, as usual, in dimensionless form, as Sherwood number:

$$Sh = \frac{kd}{D} \tag{28}$$

vs. the Graetz number:

$$Gz = \frac{u_m d^2}{DL} = \mathrm{Re}\,Sc\frac{d}{L} \tag{29}$$

Graetz in 1885 developed an infinite series solution to the analogous problem of heat transfer under the condition of constant wall temperature [Knudsen & Katz, 1958]. The solution can be immediately applied to mass transfer with constant wall concentration, simply substituting the Sherwood and Smidth numbers to the Nuselt and Prandtl numbers. The Sherwood number approaches the limiting value Sh_∞=3.66 for low Graetz number, i.e. for long distance.
In the entry region (low distance) the Leveque approximation can be applied. It assumes that concentration gradients are limited to a thin layer near the wall. The result in term of average Sherwood number is:

$$Sh_0 = 1.615 \;\; Gz^{1/3} \tag{30}$$

All the relations reported in this work give the average Sherwood numbers, which are useful for design purposes. It should be remember that, in the entry zone, the local Sherwood number is 2/3 of the average value.
An interpolating formula is currently used instead of the infinite series solution for all the Graetz numbers [Knudsen & Katz, 1958]:

$$Sh = 3.66 + \frac{0.0668 \quad Gz}{1 + 0.04 \quad Gz^{2/3}} \tag{31}$$

An alternative expression for all the Gz values can be obtained combining the two asymptotic solutions as follows [Lipinski & Field, 2001]:

$$Sh = \left(Sh_{\infty}^{n} + Sh_{0}^{n} \right)^{1/n} \tag{32}$$

Satisfactory approximation is obtained for n = 3 or 4. For n = 3 Eq. (32) simplify to:

$$Sh = \left(49 + 4.21 Gz \right)^{1/3} \tag{33}$$

which can be used for all the Graetz number values, instead of the Eq. (31).
Fig. 7 reports the general behaviour: the asymptotic solution (Sh_{∞} = 3.66) is reached for Gz nearly 2, whereas the Leveque solution (entry length) applies for Gz > 50; in the transition zone Eq. (31) and Eq. (32) with n = 4 give the same results, however for large Gz Eq. (32) approaches the Leveque solution better than Eq. (31). In addition Eq. (32) can be applied not only to the present case, but to any situation in which two asymptotic solutions are available.

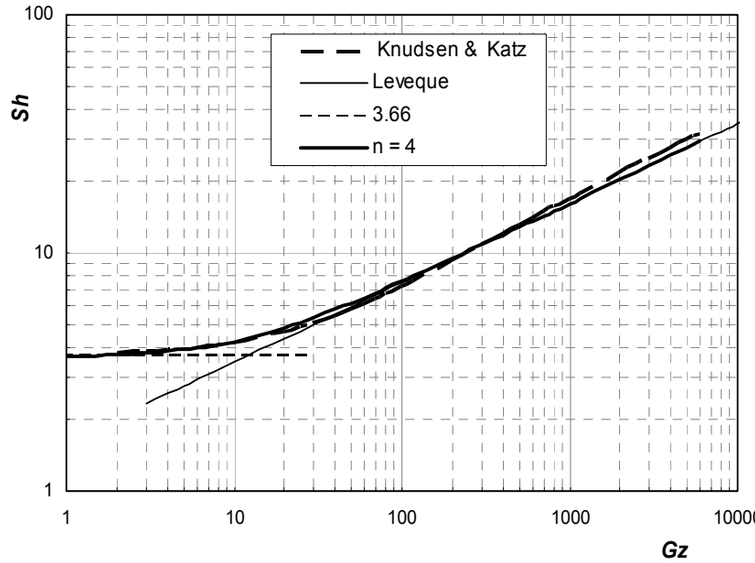

Fig. 7. Average Sherwood number vs. Graetz number for circular duct with constant wall concentration. Knudsen & Katz: Eq. (31), Leveque: Eq. (30), n = 4: Eq. (32)

Many papers suggested the use of Eq. (30), without any comment, tacitly assuming large values of Graetz Number, i.e. assuming the entry length longer than the module. This is correct in many cases, due to the low values of the diffusion coefficient in liquids; however, in very narrow hollow fibres also Graetz numbers in the transition zone are possible.
The Graez-Leveque theory showed in very good agreement with data in both heat and mass transfer experiments. Some authors reported mass transfer coefficients lower than the predictions at low flows (Gz<10). This is attributed to the slight polydispersity of the hollow

fibre diameters, which produces uneven flows [Wickramasinghe et al., 1992; Kreulen et al., 1993]. This effect is not relevant at larger flows.
The Graetz problem was solved also under the conditions of uniform wall flux; in the entry zone the expression similar to Eq. (30) is

$$Sh_0 = 1.953 \ \ Gz^{1/3} \tag{34}$$

whereas for long distance, i.e. low Graetz Number, the asymptotic value is Sh_∞=4.36. These values are nearly 20% larger than the Sherwood number calculated in the conditions of constant wall concentration. What condition better applies to the real situation can be questionable.

4.2 Mass transfer in the shell side

The calculation of shell side mass transfer coefficient is subject to more uncertainties, with respect to lumen side; correlations derived from experiments give different results and are often effective only for a specific module geometry and flow configuration, and thus are not very useful for evaluating new module designs [Lemanski & Lipscomb, 2001].
The theoretical models proposed can be roughly classified in the following categories i) regular packing of fibres, ii) single fibre, ii) random packing of fibres. The main features of the models will be briefly reviewed in the following.
Of interest to the problem at hand are also investigations of heat transfer in shell-and-tube exchangers in laminar flow. [Sparrow et al., 1961], developed an analytical solution to the governing equations for regular triangular and square tube arrangements with uniform wall heat flux. In an early work the same authors [Sparrow & Loeffler, 1959] derived the actual velocity profile for laminar flow between cylinders arranged in regular triangular or square arrays. Both the flow pattern and pressure drop depends strongly on the type of array for small spacing between the cylinders, but become independent of it for large spacing. Under these circumstances the velocity distribution around any one tube can be considered cylindrically symmetrical, so that an "equivalent annulus" model can be adopted, in which flow take place in a fictitious annular duct, which approximates the actual polygonal area surrounding each tube, as depicted in Fig. 8

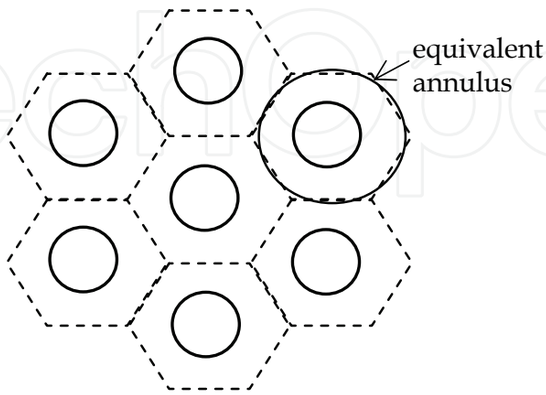

Fig. 8. The equivalent annulus approximation

Sparrow et al. showed that this simplified model can be used to describe the heat transfer for large spacing. For low spacing the model predicts asymptotic Nusselt numbers grater

than the actual ones for triangular array. From these results one can infer that the annulus model is reasonable for membrane contactors in which the fibres are not too closely spaced.
Shell side heat transfer in shell-and-tube exchangers in laminar flow were also modelled by [Miyatake & Iwashita, 1990] for triangular and square tube arrangements, but under the conditions of uniform wall temperature. The Authors developed a finite difference solution to the governing equations and presented correlations covering a broad range of Graetz numbers. Their correlations can be easily adapted to the equivalent mass transfer problem, see [Kreulen et al., 1993; Asimakopoulou & Karabela, 2006] who presented the modification for mass transfer as appendix of their works.
The comments are similar to the previous ones: heat (mass) transfer coefficients depends on the type of array for large packing density, but is almost independent of it for packing fraction less than 0.5; in this conditions the equivalent annulus formulation can be used with confidence.
A further condition for the validity of the annulus mode is a uniform distribution of the fluid, so that each fibre works in the same manner. This is an obvious, but rarely realised goal in module manufacture.
In real modules the hollow fibres are packed randomly rather than in regular array. Nevertheless, if the packing density is low, the random arrangement does not seriously invalidate the annulus model. In fact, for large spacing the flow pattern is actually independent of the type of array. Furthermore for a high packing density mass transfer is probably limited by channelling of the fluid through the irregularly arranged fibres. Therefore, it is questionable if greater accuracy would be provided by a more complicated model in which a regular array is assumed and peripheral variations are taken into account.
At this point we can say that the equivalent annulus formulation has to be preferred, for its simplicity, to models based on regular arrangement of fibres for low packing density. For high packing density (ϕ>0.5) probably the model fails, but models based on regular arrangement are expected to not work better.

4.2.1 The equivalent annulus formulation

The model assumes that around each tube, the flow take place in an annular duct bounded by a free surface of diameter d_a chosen so that the overall flow area is identical to that of the actual configuration, Fig. 9.

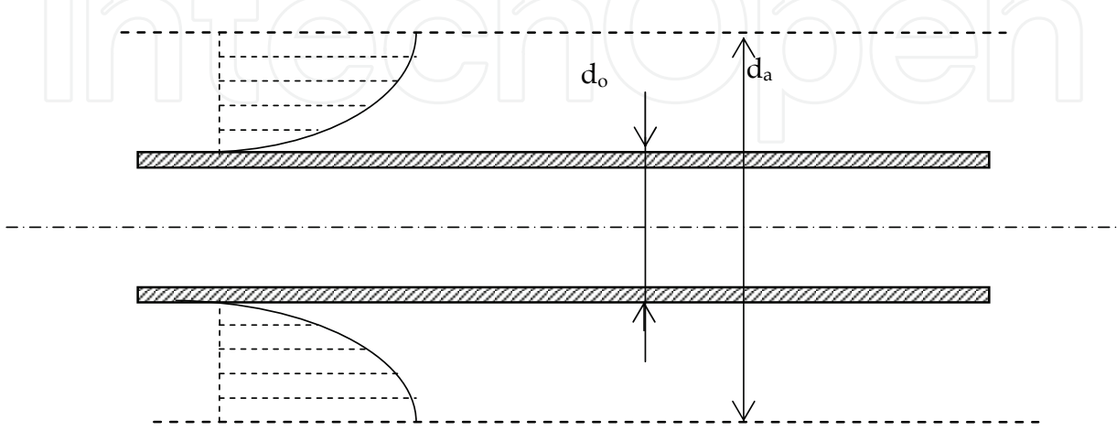

Fig. 9. A fibre with the surrounding fictitious annular duct

The outer diameter of the annulus is thus related to the packing fraction by:

$$d_a = \frac{d_o}{\sqrt{\phi}} \tag{35}$$

The maximum value $\phi = 0.9$ correspond to the situation in which the fibres are tangent to one other in a triangular array. As discussed before as ϕ approaches this value the model becomes inappropriate.

The velocity profile for fully developed laminar flow in the fictitious annular duct has been obtained by solving the equation of motion with the boundary conditions of zero velocity at the tube wall ($r = R_o = d_o/2$) and zero momentum flux at the external surface of the annulus ($r = R_a = d_a/2$). The velocity profile is given by:

$$u_{(r)} = \frac{u_m}{f(\phi)}\left[\ln\frac{r}{R_o} - \frac{\phi}{2}\left(\frac{r^2}{R_o^2} - 1\right)\right] \tag{36}$$

In which u_m is the average velocity, related to the pressure gradient by:

$$u_m = -\frac{1}{2\mu}\frac{dP}{dz}R_a^2 f(\phi) \tag{38}$$

And:

$$f(\phi) = \frac{\ln(1/\phi)}{2(1-\phi)} - \frac{3-\phi}{4} \tag{39}$$

It can be easily shown that Eq. (36) is equivalent to that obtained by Happel [Happel, 1959] for the so called "free surface model", one other name of the equivalent annulus model here described.

The steady state differential mass balance equation is

$$u_{(r)}\frac{\partial C}{\partial z} = D\frac{1}{r}\frac{\partial}{\partial r}\left(r\frac{\partial C}{\partial r}\right) \tag{40}$$

In which $u_{(r)}$ is local velocity, given by Eq. (36), D the diffusion coefficient, C the concentration of the diffusing species and z the axial coordinate.

Asymptotic solution for low z values (the entrance zone) can be obtained following the Leveque procedure, i.e. assuming that concentration gradient in the fluid are limited to a thin layer near the wall. Under the condition of constant wall concentration the average Sherwood number is:

$$Sh = 1.0178\left[\frac{1-\phi}{f(\phi)}\right]^{1/3} Gz^{1/3} \tag{41}$$

In which the Sherwood and Graetz numbers are defined making reference to the outer diameter of the tubes as characteristic length:

$$Sh = \frac{kd_o}{D} \quad Gz = \frac{u_m d_o^2}{Dz} \tag{42}$$

It will be noted that in the range 0.1 < ϕ <0.6 the above equation (41) can be represented, with accuracy better than 99% by the expression linear in ϕ:

$$Sh \approx (1+2\phi)Gz^{1/3} \tag{43}$$

In passing also the Leveque-type solution under the condition of uniform wall flux is reported for completeness:

$$Sh = 1.23\left[\frac{1-\phi}{f(\phi)}\right]^{1/3} Gz^{1/3} \tag{44}$$

The complete solution of Eq. (40) under the conditions of constant wall concentration was obtained by a finite difference method and is represented in Fig. 10 as average Sherwood number vs. Graetz number for different values of the packing fraction. Of course the numerical solution approaches the asymptotic solution, Eq. (41), for large Gz values, i.e. in the entrance zone, where the Leveque approximation applies. In Fig. 10 is also reported a line representing the Gz values above which the actual Sh differ less than 1% from the values calculated from Eq. (41), valid in the entrance zone. That line is represented by the interpolating formula:

$$Gz_{\lim} = 58\, e^{6.3\,\phi} \tag{45}$$

Apparently the length of the entry zone strongly depends on the packing fraction, ranging from nearly Gz = 100 for ϕ = 0.1, to Gz =2500 for ϕ = 0.6.

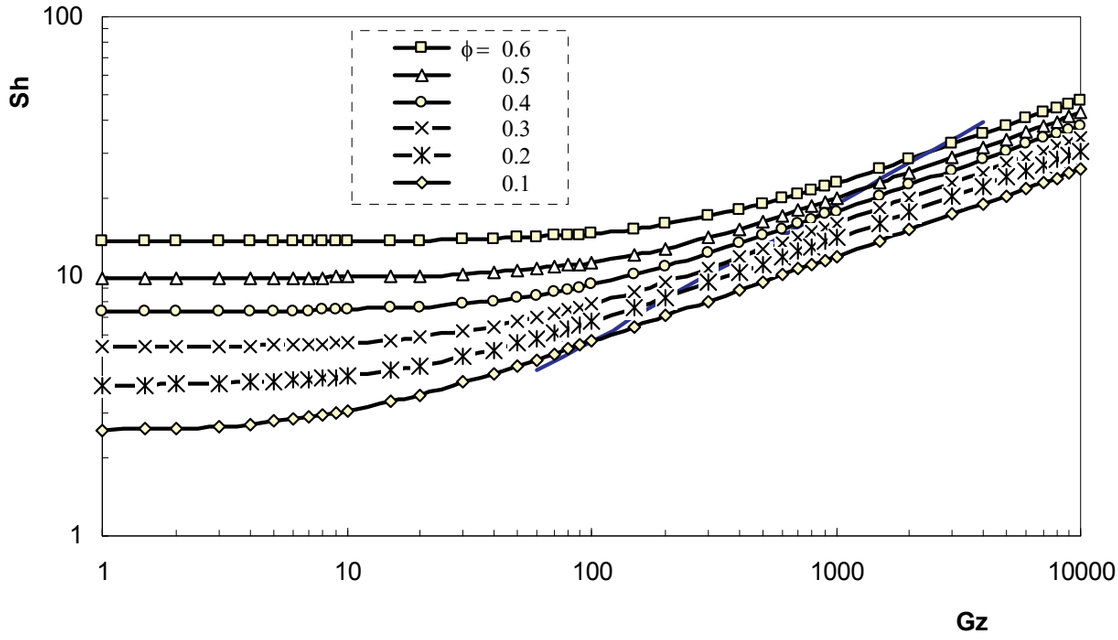

Fig. 10. Average Sherwood numbers for the equivalent annulus model under the conditions of constant wall concentration, for different values of the packing fraction ϕ

Fig. 10 shows that limiting values of Sh are approached for long distance, i.e. for low Graetz numbers. The dependence of these limiting values on the packing fraction ϕ, in the range $0.1<\phi<0.6$, is well described by the interpolation formula:

$$Sh_{\infty} = 1.93\, e^{3.29\,\phi} \tag{46}$$

The same qualitative behaviour was already observed for the solution of Eq. (40) under the conditions of uniform wall flux. In that case is possible to develop an analytical asymptotic solution also for large z values, i.e. low Gz, following a procedure similar to that reported in [Bird et al, 2007] for circular channel. The complete analytical solution was reported elsewhere [Gostoli & Gatta, 1980]. A more handy interpolation formula, for the range $0.1<\phi<0.65$, is here reported:

$$Sh_{\infty} = 2.08\, e^{3.3\,\phi} \tag{47}$$

The two solutions for low Graetz numbers are reported in Fig. 11, together with the data for triangular array, after [Miyatake & Iwashita, 1990]. Apparently the equivalent annulus formulation gives practically the same results as the more elaborated model of triangular array for packing fraction ϕ less than 0.45; only for larger packing fraction the deviation becomes substantial.

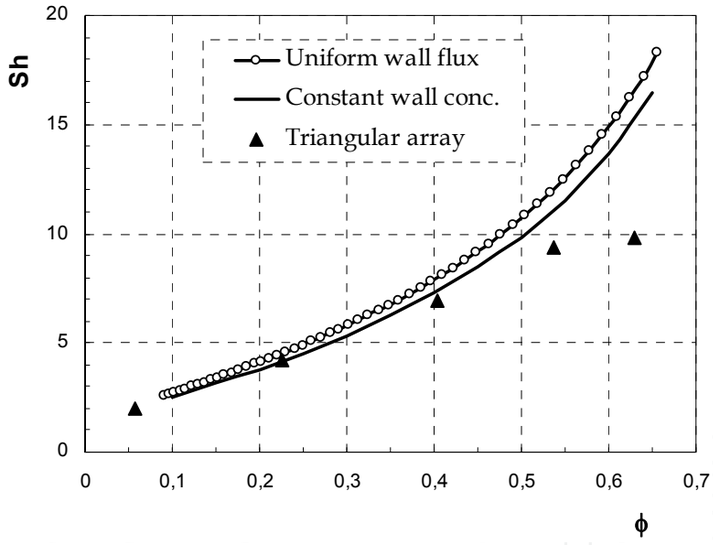

Fig. 11. Asymptotic Sherwood numbers (low Gz) for the equivalent annulus model under the conditions of uniform wall flux and constant wall concentration, compared with the data of [Miyatake & Iwashita, 1990] for triangular array

As for the tube side, a simple expression for all the Graetz number can be obtained combining the two asymptotic solutions (entrance zone and long distance) by Eq. (32).
By using n =3 in Eq. (32), Eq. (46) for long distance and the approximate expression (43) for the entrance zone the following, very handy expression is obtained:

$$Sh \approx \left[7.2\, e^{10\phi} + (1+2\phi)^3\, Gz \right]^{1/3} \tag{48}$$

which is in pretty good agreement with the numerical solution reported in Fig. 10 and can be used for practical purposes instead of the exact values.

4.2.2 Discussion

The equivalent annulus model, presented in details in the previous section, gives a simple description of the mass transfer in the shell side, leading to an approximate explicit expression for the mass transfer coefficient, the Eq. (48), very handy for design and analysis of membrane contactors. As discussed above, for packing fraction up nearly 0.45, the model gives the same results of the more complicated models of regular arrangement in which the circumferential dependence of velocity and concentration are taken into account.

Of course its adequacy to describe mass transfer in actual apparatuses can be questioned.

The equivalent annulus model was compared to experimental results in [Asimakopoulou & Karabelas, 2006a, 2006b]. In their analysis only the entry length solution, Eq. (41), was considered. In the first paper the module used contained only 5 hollow fibres of outer diameter 0.3 mm with a very low packing fraction (ϕ = 0.093) and the agreement seemed satisfactory. In the second paper, aimed to investigate the effect of packing fraction, three further modules were used with packing fraction up to 0.4. The number of fibres contained in the modules was again quite limited, up to 68 and the modules were carefully hand made. The agreement between experiments and equivalent annulus model was again pretty good. The data showed a dependence on the packing fraction weaker than that predicted by Eq. (41), and the Authors suggested to use the simple expression $Sh = 1.45\ Gz^{0.33}$, to better represent the data in the range $0.093<\phi<0.4$. This equation corresponds to Eq. (41) or (42) for $\phi = 0.225$, i.e. nearly the average value of the packing fractions tested.

Even if limited to the Leveque-type solution (the entrance zone), essentially the works of Asimakopoulou and Karabelas confirmed that the equivalent annulus adequately describes the mass transfer in small modules for packing fraction up to 0.4.

The situation in commercial modules, housing thousands of fibres, is somewhat more complicated. Many factors make the analysis complex and uncertain [Bao & Lipscomb, 2003]: 1) fibres are packed randomly in the module, 2) the fibres may not lie parallel to each other leading to a transverse flow component, 3) cross-flow regions are present near the entrance and exit ports, 4) fluid distribution into the bundle may not be uniform if the entrance and exit ports are not well designed. Finally the fibres are flexible and the arrangement may change with the flow.

Only the first factor, the effect of random fibre packing, received considerable attention. [Zheng et al, 2004] described the effect of randomness by a generalized free surface model, introducing a probabilistic distribution for the areas of the fictitious annuli circumventing each fibre. [Wu & Chen, 2000] used Voronoi tessellation to generate polygonal regions around each fibre. [Bao & Lipscomb G., 2002] modelled the fibre bundle as an infinite, spatially periodic medium. All the results indicate that channelling through randomly packed bundles reduces the average mass coefficient relative to regularly packed bundles, especially in the well developed limit.

A number of experimental correlations for shell side mass transfer appeared in literature, [Lipnizki & Field, 2001] provide an excellent summary and discussion. These correlations predict values that can be either much higher or much lower than the values calculated for regular and random fibres packings. This suggests that the other factors mentioned above can control the flow field. The presence of cross-flow regions due to shell port design or

non-parallel fibres may lead to higher than expected mass transfer coefficients. Poor fluid distribution may lead to lower than expected values. A number of apparent errors in the literature experimental correlations were also pointed out [Liang & Long, 2005].
The comparison of the models and correlations is also complicated by the different parameters used to characterize the packing as well as the different definition of the characteristic diameter. In this paper the outer fibre diameter d_o has been used in the definition of Reynolds and Sherwood numbers; many authors instead used the hydraulic diameter d_h, which depends on the packing fraction:

$$d_h = d_o\left(\frac{1}{\phi} - 1\right) \tag{49}$$

Both choices can be accepted, the outer diameter seems more rational to compare the performances of modules made with the same fibres, but with different packing density.

5. Biosynthetic vanillin

Vanillin (4-hydroxy-3-methoxy-benzaldehyde), the major organoleptic component of natural vanilla, is the most widely used flavour compound in food, cosmetics and pharmaceutical industries [Guzman, 2004]. Natural vanillin, obtained from *Vanilla* pods through a long and expensive process, can supply less than 1% of the market demand. Therefore, most of the vanillin employed is obtained through chemical synthesis from guaiacol or lignin [Ramachandra & Ravishankar, 2000]. The production of vanillin through microbial or enzymatic bioconversion of selected substrates such as ferulic acid or capsaicin is an interesting alternative, as the product can be labelled as "natural" according to the European and US legislation. Studies regarding the production of biotechnological vanillin have shown that several microorganisms have the potential of being used in the bioconversion of ferulic acid into vanillin, such as actinomycetes, *Pseudomonas spp., Bacillus spp*. and *Aspergillus spp.* [Walton et al., 2000]. Vanillin can also be obtained by an enzymatic process from capsaicin in two steps: capsaicin is converted by acilase to vanillylamine, which is then converted to vanillin by amine oxidase. [van den Heuvel et al., 2001]
The recovery of the product from the bioconversion broth is a key point of the whole process. As vanillin has toxic effect on bacterial cells and it can be further transformed to vanillyl alcohol or vanillic acid, the productivity can be potentially enhanced by in-situ removal of vanillin. The addition of adsorbent resins to the culture medium was proposed in the biotransformation of ferulic acid to vanillin by a *Streptomyces* sp. strain [Dongliang et al., 2007] in a fed-batch process. Pervaporation was also a proposed for product removal [Boddeker et al., 1997], however, owing to the low volatility, the vanillin flux was quite low at the bioconversion temperature. The aim of this work is to evaluate the potential of using membrane contactor technology for the recovery of vanillin from bioconversion broths in view of an integrated bioconversion – separation process.

6. Experimental

The partition coefficients of vanillin as well as of the substrates of the bioconversion (ferulic acid and vanillylamine) in various solvents were determined through batch experiments. The solvent selected was n-butyl acetate. This solvent allows the selective removal of the

produced vanillin from the bioconversion broth removing only a minor extent of the substrates. Indeed the partition coefficient of vanillin is 21 (at pH 7) whereas for ferulic acid it is 0.2 and for vanillylamine 0.01. As shown in Tab 2, the partition coefficient of vanillin depends on pH, making possible to counter-extract vanillin from the vanillin rich solvent phase by using alkaline water.

pH	7	8	9	10	12
m	21	15.8	10.4	4.4	0.02

Table 2. Partition coefficient of Vanillin between water and n- butyl acetate at various pH

Accurel® polypropylene hollow fibres, supplied by Membrana GmbH, Germany, with inner/outer diameter 0.6/1 mm and porosity 60% were used to build the module used in the experiments. The module contained 30 hollow fibres with overall area 158 cm^2 , the shell diameter was 10 mm, the packing fraction was thus $\phi = 0.3$.

The experimental set up is shown schematically in Fig. 6. The feed and the solvent were circulated counter-currently through the module and the respective reservoirs by two gear pumps with variable speed. The pressure of aqueous phase was kept a bit larger than that of the organic phase; to this purpose the feed reservoir was kept at a higher level with respect to the solvent reservoir. In addition a suitable overpressure (0.2-0.4 bar) can be created by a valve at the module exit. Both circuits were equipped with instruments for measuring the temperature and the flow rate during the experiments.

Small samples of the organic and aqueous phases were taken at various times and analyzed with HPLC reverse phase system, equipped with a Beckman Ultrasfere 4.6 mm x 250 mm ODS C18 column (particle diameter = 5 μm) , at 35°C. The mobile phase was composed of 70% H_20 added with 1% CH_3COOH and 30% CH_3OH added with 1% CH_3COOH; column temperature was 35°C, injection volume was 20 μL. The isocratic elution was performed for 16 minutes.

Four type of extraction experiments were performed: i) extraction from model solutions containing vanillin and ferulic acid or vanillylamine (the substrates of microbial and enzymatic conversion respectively), ii) extraction from the whole bioconversion broth, iii) extraction during bioconversion coupling bioconversion and separation, iv) counter-extraction of vanillin from the solvent by NaOH-water solution. The feed flowed either through the lumen or in the shell side. In all the experiments the temperature was 30°C and the pH was 7 in the extraction experiments and 12 in the counter extraction.

The bioconversion broth used in the experiments was obtained in a 3.5 L stirred tank bioreactor by *Pseudomonas fluorescens* BF13-1p at concentration 6 g/L with ferulic acid (2 g/L) as unique carbon source, at 30°C and pH 7.

7. Results

Typical results obtained in the extraction experiments are shown in Figs 12 and 13, in the first case the aqueous solution contained vanillin and ferulic acid, in the second one vanillin and vanillylamine.

Apparently vanillin was rapidly removed and reached the concentrations corresponding to the partition coefficient measured in batch experiments, whereas the ferulic acid or vanillylamine concentrations in the aqueous phase remained almost constant. The membrane

based solvent extraction is thus a good technique for the selective removal of vanillin without removing the substrates of the bioconversion.

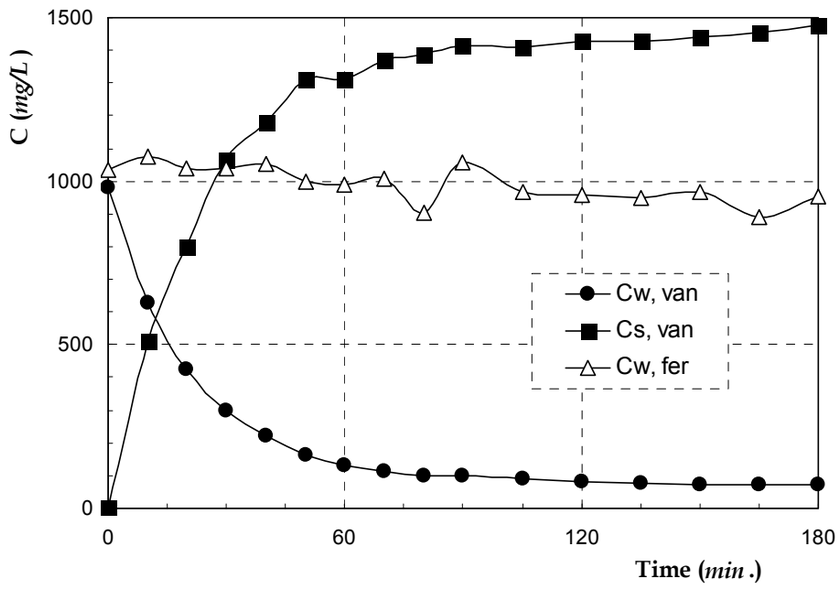

Fig. 12. Vanillin and ferulic acid concentrations vs. time in the extraction with buthyl-acetate. Feed shell side, feed volume 0.5 L, solvent volume 0.3 L, feed flow rate 45 L/h, solvent flow rate 25 L/h, pH 7

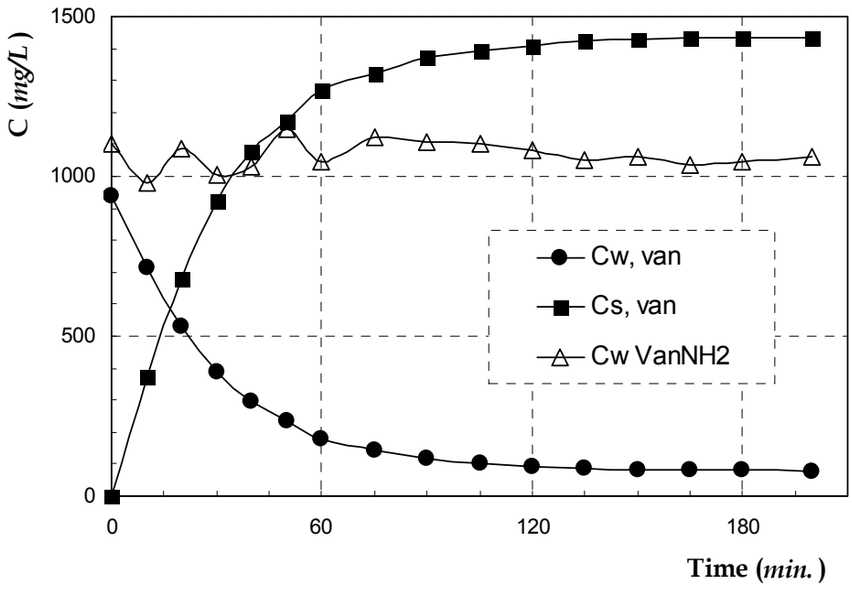

Fig. 13. Vanillin and vanillylamine concentrations vs. time in the extraction with buthyl-acetate. Feed shell side, feed volume 0.5 L, solvent volume 0.3 L, feed flow rate 45 L/h, solvent flow rate 25 L/h, pH 7

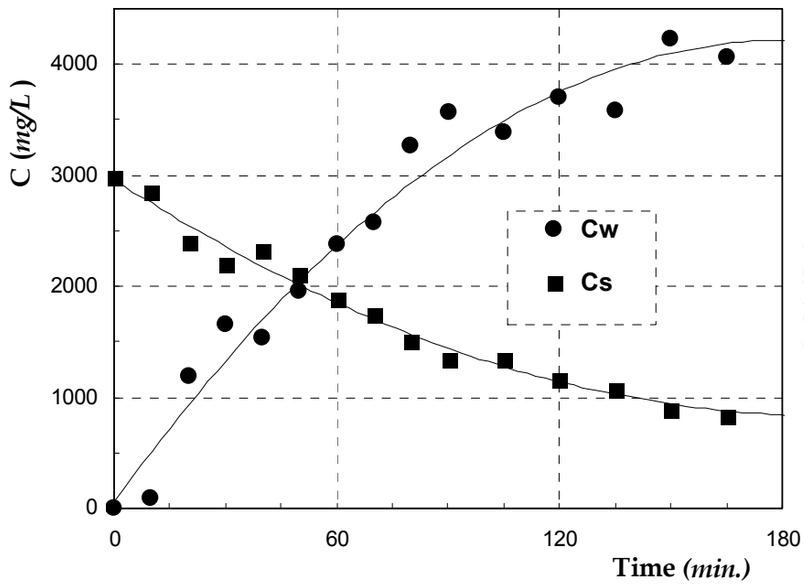

Fig. 14. Vanillin concentration in the organic and aqueous phases vs. time in the counter extraction from buthyl-acetate to water at pH = 12. Solvent tube side, solvent volume 0.5 L, water volume 0.3 L, solvent flow rate 25 L/h, feed flow rate 45 L/h

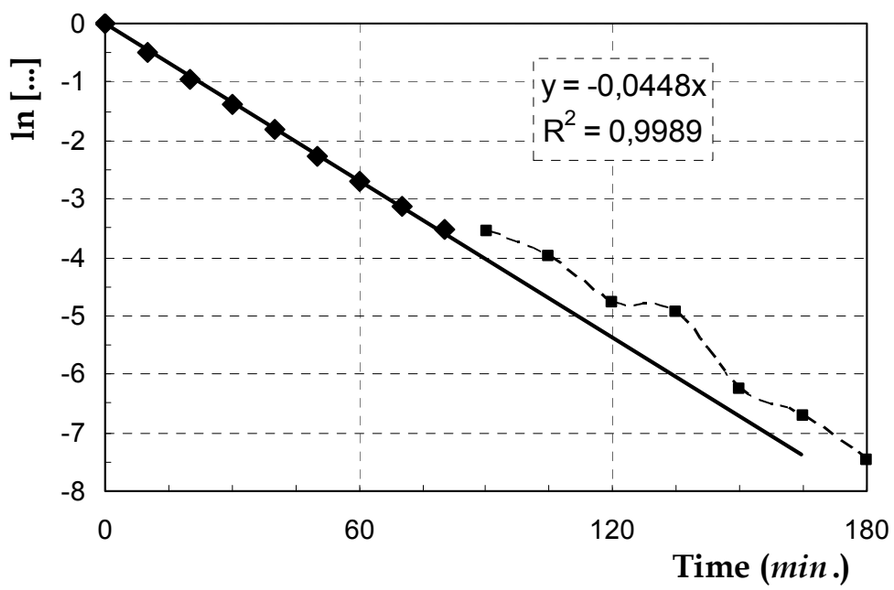

Fig. 15. Evaluation of the module efficiency through Eq. (20); same data as Fig. 13

Fig 14 refers to a counter-extraction experiment at pH 12, and reports the time course of the vanillin concentration in the organic and in the aqueous phases. Due to the favourable partition coefficient vanillin effectively moved towards the aqueous phase. The mass transfer was somewhat slower than in the extraction runs performed in similar conditions,

this behaviour can be clearly explained considering that, in this case, due to the partition coefficient value, the mass transfer resistance through the membrane was quite large.
The module efficiency was calculated from the vanillin concentration vs. time data as explained in the theoretical section (paragraph 3.1), i.e. plotting the left side of Eq. (20) vs. time. As shown in Fig. 15, which reports to the same data of Fig. 13, the data were well fitted by a straight line, of course only the points sufficiently apart from the equilibrium were considered, up to 90 minutes of experiment in this case.
From the slope of the straight (*0.0448*) the efficiency was calculated to be E_{ff} = *2.8 %*, finally the overall mass transfer coefficient, calculated from Eq. (15) was K_w = *1.3 10-5 m/s*.
Tab. 3 summarizes the results obtained in the same way for all the extraction experiments. There is a pretty good agreement between the experimental and theoretical values of the mass transfer coefficients, which of course refers to the actual interface, the inner surface for aqueous feed flowing through the lumen, and the outer surface for aqueous feed in the shell.

W *(L/h)*	S *(L/h)*	η *%*	K_w *(m/s)*	$K_{w\ theor}$ *(m/s)*
Feed tube side				
12	10	4.76	$1.4\ 10^{-5}$	$1.45\ 10^{-5}$
20	20	5.36	$1.6\ 10^{-5}$	$1.62\ 10^{-5}$
45	25	2.0	$1.5\ 10^{-5}$	$1.98\ 10^{-5}$
Feed shell side				
20	35	4.52	$9.7\ 10^{-6}$	$7.6\ 10^{-6}$
45	25	2.77	$1.3\ 10^{-5}$	$9.2\ 10^{-6}$

Table 3. Module efficiency, experimental and theoretical values of the mass transfer coefficients in the extraction runs at different aqueous phase and solvent flow rates

The mass transfer coefficients were lower for feed flowing shell side with respect to the feed flowing through the lumen; however, it has to be considered that the interfacial area is substantially larger in the latter case, being the external surface of the fibres. As a result the mass transfer rates were comparable in the two cases.
The relative role played by the various mass transfer resistances involved were estimated from Eqs (25) or (26) based on the theoretical values of the individual mass transfer coefficients. In all cases the main resistance was associated to the aqueous phase boundary layer (70-80%). The membrane resistance too was appreciable (20-25%) while the solvent boundary layer played a minor role.
As expected, behaviour is different in counter-extraction. From the data of Fig. 14, the module efficiency was calculated to be nearly 0.9 and the membrane is responsible for 95% of the overall resistance; the solvent boundary layer played a minor role (nearly 5 %), whereas the aqueous phase mass transfer resistance was completely negligible. Of course in the counter-extraction hydrophilic membranes would be more convenient than the hydrophobic membranes used in this work.
Extraction experiments with the whole bioconversion broth gave nearly the same results, showing that fouling did not represent a serious problem. The coupling of the membrane contactor with the bioreactor exhibited good results for the enzymatic conversion of vanillylamine to vanillin. Fig. 16 reports one test performed as follows: in the first period

(up to 180 min) enzymatic conversion was performed in a conventional stirred tank reactor, the reactor was then connected to the hollow fibre module (as in Fig. 6). Apparently the vanillin was quickly transferred to the solvent and the reaction (vanNH2 → vanillin) proceeded with the same kinetics.

The results were not equally successful in the case of microbial conversion of ferulic acid to vanillin. After the start up of the extraction, the microbial activity seemed to stop almost at all. May be the solvent had a strong inhibitory effect, or the solvent itself was used as a substrate instead of ferulic acid; this point require further investigations.

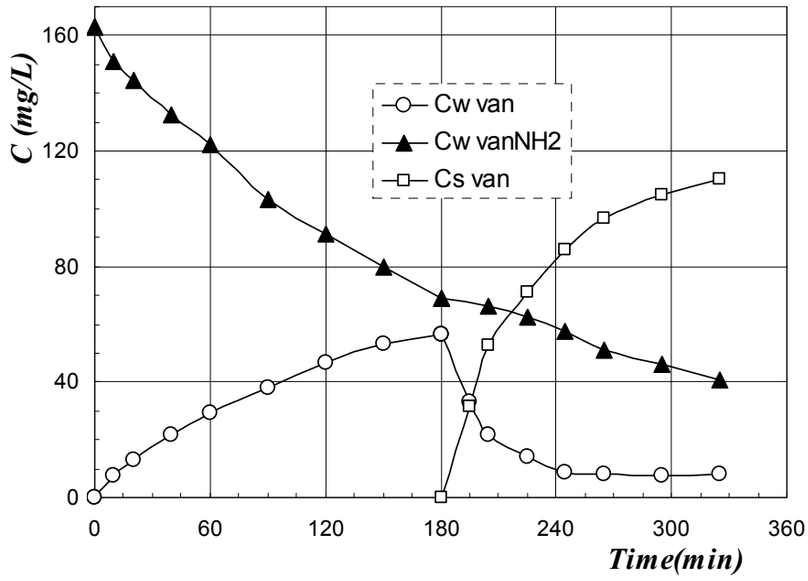

Fig. 16. Coupling extraction and enzymatic conversion

8. References

Asimakopoulou, A.G. & Karabelas, A.J., (2006a). Mass transfer in liquid–liquid membrane-based extraction at small fiber packing fractions, *Journal of Membrane Science* 271,151–162.

Asimakopoulou, A.G. & Karabelas, A.J., (2006b). A study of mass transfer in hollow-fiber membrane contactors - The effect of fiber packing fraction. *Journal of Membrane Science* 282, 430-441

Bao, L. & Lipscomb G.G., (2002). Mass transfer in axial flows through randomly packed fiber bundles with constant wall concentration, *Journal of Membrane Science* 204, 207–220

Bao, L. & Lipscomb G. G. (2003). Mass transfer in axial flows through randomly packed fiber bundles, In: *New Insights into Membrane Science and Technology: Polymeric and Biofunctional Membranes,* Bhattacharyya D. & Butterfield D.A. (Editors), pp. 5 – 26, Elsevier Science B.V., ISBN: 0-444-51175-X, Amsterdam.

Bird, R.B., Stewart, W.E. & Lightfoot, E.N. (2007). *Transport Phenomena*. John Wiley & Sons. ISBN: 978-0-470-11539-8, New York.

Boddeker, K.W; Gatfield, I.L.; Jahnig J. & Schorm C. (1997). Pervaporation at the vapor pressure limit: Vanillin, *Journal of Membrane Science* 137, 155-158.

D'Elia, N.A., Dahuron, L., Cussler, E.L., (1986). Liquid-Liquid extraction with microporous hollw fibres, *Journal of Membrane Science* 29, 309-319.

Devis H.R. & Parkinson G.V. (1970). Mass transfer from small capillaries with wall resistance in laminar flow regime, *Applied Sci. Research* 22(1), 20 – 30.

Ding,W.; He, L.; Zhao, G.; Zhang,H; Shu, Z.; Gao, D. (2004). Double porous media model for mass transfer of hemodialyzers. *International Journal of Heat and Mass Transfer* 47, 4849–4855.

Dongliang H.; Cuiqing, M.; Song ,L.; Lin, S.; Zang, Z.; Deng, Z. & Xu, P. (2007). Enhanced vanillin production from ferulic acid using adsorbent resin, *Appl. Microbiol Biotechnol* 74, 783-790

Drioli, E.; Criscuoli, A. & Curcio E. (2006). *Membrane contactors: fundamentals, applications and potentialities*, Elsevier, ISBN 0-444 52203 4, Amsterdam

Frank, G.T. & Sirkar, K.K. (1987). An integrated bioreactor-separator: in situ recovery of fermentation products by a novel membrane-based dispersion free solvent extraction technique. *Biotechnology and Bioengineering Symp*. 17, 303 - 316

Gaeta, S.N, 2003. Membrane contactors in industrial applications. Proc. of 1st Italy-Russia Workshop on membrane and membrane processes, Cetraro (I), 51-55

Gawronski, R. & Wrzesinska , B. (2000). Kinetics of solvent extraction in hollow-fiber contactors. *Journal of Membrane Science* 168 , 213–222

Gostoli, C. & Gatta A. (1980). Massa transfer in a hollow fiber dialyser, *Journal of Membrane Science* 6, 133 – 148.

Guzman, C. (2004). Vanilla, In *Handbook of herbs and spices, Vol. 2*, Peter K.V. (Ed.), pp. 322 – 354, Woodhead Publishing, ISBN: 1-85573-721-3, Cambridge, UK.

Happel, J. (1959). Viscous flow relative to arrays of cylinders. *AIChE Journal* 5, 174 – 177.

Hatton A.P. & Quarmby (1962). Heat transfer in the thermal entry length with laminar flow in annulus, *International Journal of heat and mass transfer* 5(19), 973 -980.

Knudsen, J.G. & Katz, D.L. (1958).*Fluid dynamics and heat transfer*, McGraw-Hill, ISBN, New York.

Koonaphapdeelert, S.; Li, K. (2007). Preparation and characterization of hydrophobic ceramic hollow fibre membrane. *Journal of Membrane Science* 291 (1–2), 70–76.

Koonaphapdeelert, S.; Zhentao Wu & Li, K. (2009). Carbon dioxide stripping in ceramic hollow fibre membrane contactors, *Chemical Engineering. Science*. 64, 1 - 8

Kosaraju, P.B. & Sirkar, K.K. (2007). Novel solvent-resistant hydrophilic hollow fiber membranes for efficient membrane solvent back extraction. *Journal of Membrane Science* 288, 41–50.

Koschilowski, J.; Wieghaus M. & Rommel M. (2003). Solar thermal driven desalination plants based on membrane distillation. *Desalination* 156, 295-304.

Kreulen, H.; Smolders, G.F.; Versteeg, G.F. &van Swaaij W.P.M. (1993). Microporous hollow fibre membrane modules as gas-liquid contactors. *Journal of Membrane Science* 78, 197-216.

Lazarova, Z., Syska, B. & Schugerl, K. (2002). Application of large scale hollow fiber membrane contactors for simultaneous extractive removal and stripping of penicillin G. *Journal of Membrane Science* 202, 151 – 164.

Li, K. (2007). Ceramic membranes for separation and reaction. *John Wiley,* ISBN 978-470-01440-0, Chichester.

Lemanski, J. & Lipscomb, G.G. (1001). Effect of shell-side flows on the performance of hollow-fiber gas separation modules. Journal of Membrane Science 195, 215–228.

Liang, T. & Long, R.L. (2005). Corrections to Correlations for Shell-Side Mass-Transfer Coefficients in the Hollow-Fiber Membrane (HFM) Modules. *Ind. Eng. Chem. Res. 44,* 7835-7843.

Lipnizki, F. & Field, R.W. (2001) Mass transfer performance for hollow fibre modules with shell-side axial feed flow: using an engineering approach to develop a framework, *Journal of Membrane. Science* 193, 195–208.

Lv, Y.; Yu, X.; Jia J.; Tu, S.T.; Yan, J. & Dahlquist, E. (2011). Fabrication and characterization of superhydrophobic polypropylene hollow fiber membranes for carbon dioxide absorption. *Appl Energy* doi:10.1016/j.apenergy.2010.12.038

Miyatake, O. & Iwashita, H. (1990). Laminar-flow heat transfer to a fluid flowing axially between cylinders with a uniform surface temperature, *Int. J. Heat Mass Transfer* 33 (3) 417–425

Nunge, R.J. & Gill W.N. (1966). An analytical study of laminar counter flow of double-pipe heat exchanger, *AIChE Journal* 12, 279 – 289.

Ramachandra Rao S. & Ravishankar G.A. (2000). Vanilla flavour: production by conventional and biotechnological routes. *J Sci Food Agric;* 80, 289-34

Reid R.C.; Prausnitz J.M. & Poling B.E. (1978) "*The properties of gas & liquids*", McGraw-Hill. ISBN 0-07-100284-7, New York.

Seara, J.F.; Uhìa F.J.; Jaime Sieres, J.S. & Campo, A. (2007). A general review of the Wilson plot method and its modifications to determine convection coefficients in heat exchange devices. *Applied Thermal Engineering* 27 2745–2757.

Schlosser, S.; Kertész, R. & J. Martàk J. (2005). Recovery and separation of organic acids by membrane-based solvent extraction and pertraction. An overview with a case study on recovery of MPCA. *Separation and Purification Technology* 41, 237–266.

Siegel, R.; Sparrow, E.M. & Hallman T.M. (1958). Steady laminar heat transfer in circular tube with prescribed wall heat flux, *Applied Sci. Research* A7(5), 386 – 392.

Sparrow, E.M. & Loeffler, A.L. (1959). Longitudinal laminar flow between cylinders arranged in regular array. *AIChE Journal* 5, 325 – 330.

Sparrow, E.M.; Loeffler, A.L. & Hubbard, H.A. (1961). Heat transfer in longitudinal laminar flow between cylinders. *Trans ASME, Journal of. Heat Transfer* 83, 415 – 422.

Trébounet, D.; Burgard, M. & Loureiro, J.M. (2006). Guidelines for the application of stationary model in the prediction of the overall mass transfer coefficient in hollow fiber membrane contactor. *Separation and purification Technology* 50, 97-106.

van den Heuvel R.H.H., Fraaije M.W., Laane C., van Berkel W.J.H., (2001) Enzymatic synthesis of vanillin, *J. Agric. Food Chem.* 49, 2954-2958.

Walton N.J., Narbad A, Faulds C.G. & Williamson G. (2000). Novel approaches to the biosynthesis of vanillin. *Curr. Opinion Biotechnol.* 11, 490-496

Wickramasinghe, S.R.; Semmens, M.J. & Cussler, E.L. (1992). Mass transfer in various hollow fiber geometries. *Journal of Membrane Science, 69, 235-250*

Wu, J. & V. Chen, V. (2000). Shell-side mass transfer performance of randomly packed hollow fiber modules, *Journal of Membrane Science*, 172, 59 – 74.

Zheng, J.M., Xu, Z.K., Li, J.M., Wang, S.Y. &Xu, Y.Y. (2004). Influence of random arrangement of hollow fiber membranes on shell side mass transfer performance: a novel model prediction. *Journal of Membrane Science* 236, 145–151

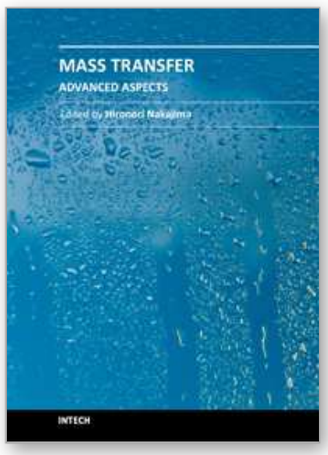

Mass Transfer - Advanced Aspects

Edited by Dr. Hironori Nakajima

ISBN 978-953-307-636-2
Hard cover, 824 pages
Publisher InTech
Published online 07, July, 2011
Published in print edition July, 2011

Our knowledge of mass transfer processes has been extended and applied to various fields of science and engineering including industrial and manufacturing processes in recent years. Since mass transfer is a primordial phenomenon, it plays a key role in the scientific researches and fields of mechanical, energy, environmental, materials, bio, and chemical engineering. In this book, energetic authors provide present advances in scientific findings and technologies, and develop new theoretical models concerning mass transfer. This book brings valuable references for researchers and engineers working in the variety of mass transfer sciences and related fields. Since the constitutive topics cover the advances in broad research areas, the topics will be mutually stimulus and informative to the researchers and engineers in different areas.

InTech Europe
University Campus STeP Ri
Slavka Krautzeka 83/A
51000 Rijeka, Croatia
Phone: +385 (51) 770 447
Fax: +385 (51) 686 166
www.intechopen.com

InTech China
Unit 405, Office Block, Hotel Equatorial Shanghai
No.65, Yan An Road (West), Shanghai, 200040, China
中国上海市延安西路65号上海国际贵都大饭店办公楼405单元
Phone: +86-21-62489820
Fax: +86-21-62489821

IntechOpen